Field distributions in curved superconducting tapes conforming to a cylinder carrying transport currents

Yasunori Mawatari
National Institute of Advanced Industrial Science and Technology (AIST), Tsukuba, Ibaraki 305-8568, Japan
(Received 29 July 2009; published 18 November 2009)

Current and magnetic field distributions in curved superconducting tapes are investigated theoretically. The geometry of superconducting tapes considered here is a section of a cylindrical shell in which the length of tape lies parallel to the long axis of the cylinder. Analytical investigation based on the critical state model demonstrates that the current and field distributions and the ac losses in curved superconducting tapes carrying transport currents are equivalent to those in an infinite array of coplanar superconducting tapes. Bending a superconducting tape reduces the magnetic field perpendicular to the tape, resulting in a reduction of ac losses. Simple analytical formulas are presented for the hysteretic ac losses in curved superconducting tapes carrying ac transport currents.

DOI: 10.1103/PhysRevB.80.184508 PACS number(s): 84.71.Mn, 74.25.Nf, 74.25.Ha, 74.25.Sv

I. INTRODUCTION

Electromagnetic responses (e.g., current and magnetic field distributions and ac losses) of flat superconducting tapes [see Fig. 1(a)] have been investigated theoretically.[1–4] In a power transmission cable, however, parallel superconducting tapes wrap around a cylindrical former,[5] and the tapes can be curved conforming to the shape of the cylinder,[6] as shown in Fig. 1(b). Although such bending affects electromagnetic responses, curved superconducting tapes have not yet been investigated analytically.

In the present paper we investigate theoretically the electromagnetic response of current-carrying superconducting tapes in the shape of a section of a cylindrical shell. Analytical expressions are presented for current and field distributions and for ac losses. These theoretical results clarify the physical mechanisms of the ac losses in curved superconducting tapes and are useful for design of the configuration of power cables. The paper is organized as follows. A single isolated curved tape is investigated in Sec. II, and the case of a number of parallel curved tapes periodically arranged around a cylinder is investigated in Sec. III. The theoretical results are summarized in Sec. IV.

II. SINGLE CURVED TAPE

A. Geometry of a curved tape

In this section we consider an isolated curved superconducting tape, as shown in Fig. 1(b). The superconducting tape is curved in the xy plane and is straight and of infinite extent along the z axis. The width of the curved tape is $2w$ and the thickness is d. We consider the thin-tape limit, $d/2w \to 0$. The cross section of the curved tape in the xy plane corresponds to a circular arc of radius R and central angle $4\theta_1 = 2w/R$, as shown in Fig. 2. The flat tape corresponds to the limit $R \to \infty$ at fixed width $2w$ (i.e., $\theta_1 \to 0$).

The superconducting tape carries a transport current I_z along the z axis. First, we consider the response to a dc transport current $I_z = I_0$ which is monotonically increased from $I_z = 0$ (Sec. II B). Next, we consider the ac loss in a superconducting tape carrying an ac transport current $I_z = I_{p1} \cos \omega t$ (Sec. II C). The electromagnetic response of a curved superconducting tape is analyzed on the basis of the critical state model with constant critical current density j_c, as in the Bean model.[7] The critical current of a curved tape is $I_{c1} = 2j_c wd$.

B. Field distributions for a curved tape

The complex-field approach is a very useful and powerful method for analyzing two-dimensional magnetic fields,[8,9] where the complex field is defined as a function of $\zeta = x + iy$ by $\mathcal{H}(\zeta) = H_y(x,y) + iH_x(x,y)$. We use the conformal mapping from $\zeta = x + iy$ to $\eta = u + iv$,

$$\zeta = iR(1 - e^{i\eta/R}). \tag{1}$$

When $v = 0$, u corresponds to the arc length from $\zeta = 0$ to $\zeta = iR(1 - e^{iu/R}) = R \sin(u/R) + iR[1 - \cos(u/R)]$ on a curved tape. By using the conformal mapping of Eq. (1), a curved tape in the ζ plane (as shown in Fig. 2) is mapped onto an infinite array of coplanar tapes in the η plane (as shown in Fig. 3). In other words, the arc corresponding to the cross section of a curved tape is simply expressed as $v = 0$ and $-w + 2\pi kR < u < w + 2\pi kR$ with an arbitrary integer k.

The relationship between the complex field $\mathcal{H}(\zeta)$ in the ζ plane and the complex field $\tilde{\mathcal{H}}(\eta) = H_v(u,v) + iH_u(u,v)$ in the η plane is

$$\tilde{\mathcal{H}}(\eta) = \frac{d\zeta}{d\eta}\mathcal{H}(\zeta) = e^{i\eta/R}\mathcal{H}(\zeta). \tag{2}$$

For $v \to 0$ (i.e., $|\zeta - iR| \to R$), Eq. (2) reduces to $H_v + iH_u = e^{iu/R}(H_y + iH_x)$, which means that H_v and H_u correspond to

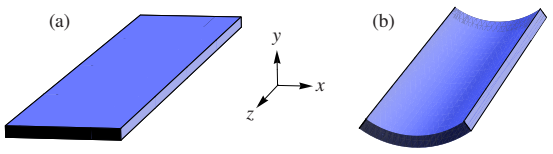

FIG. 1. (Color online) Schematic configurations of (a) a flat tape and (b) a curved tape.

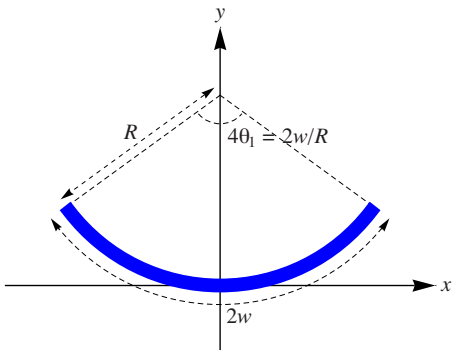

FIG. 2. (Color online) Cross section of a tape curved in the $\zeta = x+iy$ plane. This is equivalent to a circular arc of radius R (i.e., $|\zeta - iR| = R$) with central angle $4\theta_1 = 2w/R$ (i.e., $|\arg(\zeta - iR) + \pi/2| < 2\theta_1$), where $0 < \theta_1 = w/2R < \pi/2$. The limit of $\theta_1 \to 0$ corresponds to a flat tape.

the components of the magnetic field perpendicular and parallel to a curved tape, respectively.

The Biot-Savart law for complex field $\mathcal{H}(\zeta)$ and sheet current $K_z(u)$ in a curved tape is given by

$$\mathcal{H}(\zeta) = \frac{1}{2\pi}\int_{-w}^{+w} du' \frac{K_z(u')}{\zeta - iR(1 - e^{iu'/R})}. \tag{3}$$

Substituting Eqs. (1) and (3) into Eq. (2) yields

$$\tilde{\mathcal{H}}(\eta) = \frac{1}{2\pi R}\int_{-w}^{+w} du' \frac{iK_z(u')}{1 - e^{i(u'-\eta)/R}} \tag{4}$$

$$= \frac{1}{4\pi R}\int_{-w}^{+w} du' K_z(u')\left[i + \cot\left(\frac{\eta - u'}{2R}\right)\right]$$

$$= i\frac{I_0}{4\pi R} + \frac{1}{2\pi}\int_{-w}^{+w} du' K_z(u') \sum_{k=-\infty}^{+\infty} \frac{1}{\eta - u' - 2\pi kR}, \tag{5}$$

where $I_0 = \int_{-w}^{+w} K_z(u)du$ is the transport current. Equation (5) shows that $\tilde{\mathcal{H}}(\eta)$ corresponds to the complex field for an infinite array of coplanar superconducting tapes[10–12] exposed to transport currents I_0 and a parallel magnetic field $I_0/4\pi R$. The effective parallel field $I_0/4\pi R$ is smaller than the full penetration field $j_c d/2$ because $I_0 < I_{c1} = 2j_c wd$ and $R > w/\pi$. Note that the effective parallel field smaller than $j_c d/2$ does not affect seriously the electromagnetic response of superconducting tapes in the limit $d/2w \to 0$. We, therefore, can conclude that the electromagnetic response of a curved superconducting tape carrying a transport current (as shown in Fig. 2) is equivalent to that of an infinite array of coplanar tapes (as shown in Fig. 3).

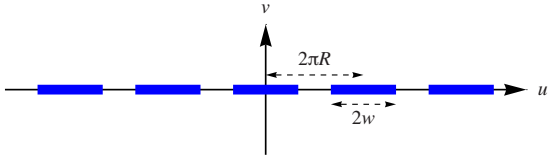

FIG. 3. (Color online) Cross section of an infinite array of coplanar tapes in the $\eta = u + iv$ plane. Coplanar tapes of width $2w$ are periodically arranged with a periodicity of $2\pi R$, and the cross section of the tapes is expressed as $v = 0$ and $|u - 2\pi kR| < w$ ($k = 0, \pm 1, \pm 2, \ldots, \pm\infty$).

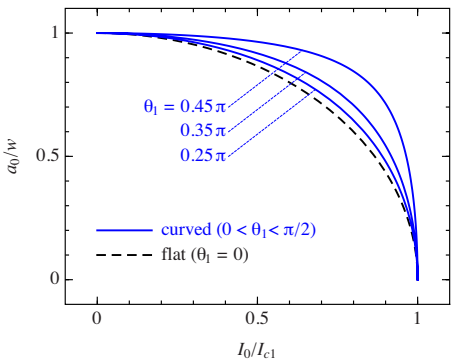

FIG. 4. (Color online) The flux front parameter, a_0, as a function of the transport current, I_0. The flux front for a flat superconducting tape with $\theta_1 = 0$ (dashed line) and for curved superconducting tapes with $\theta_1 = 0.25\pi$, 0.35π, and 0.45π (solid lines) are shown.

The current and magnetic field distributions in an infinite array of coplanar superconducting tapes have already been derived in Refs. 11 and 12. Therefore, the complex field for a curved superconducting tape $\tilde{\mathcal{H}}(\eta)$ is given by

$$\tilde{\mathcal{H}}(\eta) = \frac{j_c d}{\pi}\operatorname{arctanh}\left[\sqrt{\frac{\tan^2(w/2R) - \tan^2(a_0/2R)}{\tan^2(\eta/2R) - \tan^2(a_0/2R)^2}}\right] + i\frac{I_0}{4\pi R}, \tag{6}$$

where the parallel field component $iI_0/4\pi R$ is added for consistency with Eq. (5), and the flux front parameter a_0 is given by[11,12]

$$a_0 = \frac{w}{\theta_1}\arccos\left[\frac{\cos\theta_1}{\cos(\theta_1 I_0/I_{c1})}\right]. \tag{7}$$

Figure 4 shows plots of a_0 vs I_0 based on Eq. (7). It can be seen that the penetration of magnetic flux into a superconducting tape is delayed by its curvature.

Figure 5 shows the magnetic field lines [i.e., the contour lines of the real part of the complex potential $G(\zeta) = \int \mathcal{H}(\zeta)d\zeta = \int \tilde{\mathcal{H}}(\eta)d\eta$ from Eq. (6)] around (a) a flat superconducting tape and (b)–(d) a curved superconducting tape carrying a transport current of $I_0/I_{c1} = 0.8$.

Now we consider $\tilde{\mathcal{H}}(\eta)$ at the upper (i.e., inner) surface $\eta = u + i\epsilon$ and at the lower (i.e., outer) surface $\eta = u - i\epsilon$, where $\epsilon \to +0$ is a positive infinitesimal. The real part of Eq. (5) (i.e., the perpendicular field H_v) at $\eta = u \pm i\epsilon$ reduces to

$$H_v(u,0) = \mathrm{Re}\,\tilde{\mathcal{H}}(u \pm i\epsilon) = \frac{1}{4\pi R}\int_{-w}^{+w} du' K_z(u')\cot\left(\frac{u - u'}{2R}\right). \tag{8}$$

The imaginary part of Eq. (5) (i.e., the parallel field H_u) at $\eta = u \pm i\epsilon$ and $|u| < w$ is

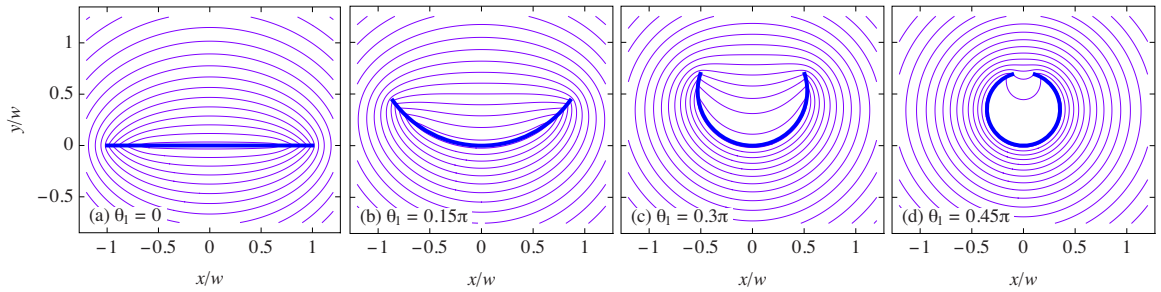

FIG. 5. (Color online) Magnetic field lines around a superconducting tape with $I_0/I_{c1}=0.8$ for $\theta_1=w/2R$: (a) $\theta_1=0$, (b) $\theta_1=0.15\pi$, (c) $\theta_1=0.3\pi$, and (d) $\theta_1=0.45\pi$. Thick lines correspond to cross sections of the superconducting tapes.

$$H_u(u,\pm\epsilon) = \mathrm{Im}\,\tilde{\mathcal{H}}(u\pm i\epsilon)$$
$$= \frac{I_0}{4\pi R} \mp \frac{1}{2}\int_{-w}^{+w} du' K_z(u') \sum_{k=-\infty}^{+\infty} \delta(u-u'-2\pi kR)$$
$$= \frac{I_0}{4\pi R} \mp \frac{1}{2}K_z(u), \tag{9}$$

where $\delta(u)$ is the delta function. Because of the curvature of the tape, the parallel field H_u is asymmetric, that is, H_u at the upper (i.e., inner) surface is smaller than that at the lower (i.e., outer) surface. In the limiting case of $\theta_1 \to \pi/2$, a curved tape becomes a hollow cylinder with a uniform sheet current $K_z=I_0/2w=I_0/2\pi R$. Then, Eq. (9) yields $H_u(u,+\epsilon)=0$ and $H_u(u,-\epsilon)=I_0/2\pi R$.

The perpendicular magnetic field component, $H_v(u,0)=\mathrm{Re}\,\tilde{\mathcal{H}}(u\pm i\epsilon)$, and the sheet current, $K_z(u)=\mathrm{Im}[\tilde{\mathcal{H}}(u-i\epsilon)-\tilde{\mathcal{H}}(u+i\epsilon)]$, derived from Eq. (6), are

$$\frac{H_v(u,0)}{j_c d/\pi} = \begin{cases} 0 & \text{for } |u|<a_0 \\ \mathrm{sgn}(u)\,\mathrm{arccoth}\,\varphi(u) & \text{for } a_0<|u|<w \\ \mathrm{sgn}(u)\,\mathrm{arctanh}\,\varphi(u) & \text{for } |u|>w, \end{cases} \tag{10}$$

$$\frac{K_z(u)}{j_c d} = \begin{cases} (2/\pi)\arctan\varphi(u) & \text{for } |u|<a_0 \\ 1 & \text{for } a_0<|u|<w, \end{cases} \tag{11}$$

where the function $\varphi(u)$ is given by

$$\varphi(u) = \sqrt{\frac{\tan^2(w/2R)-\tan^2(a_0/2R)}{|\tan^2(u/2R)-\tan^2(a_0/2R)^2|}}. \tag{12}$$

For $\theta_1 \to 0$, the respective Eqs. (6), (7), and (12) reduce to

$$\tilde{\mathcal{H}}(\eta) \to \frac{j_c d}{\pi}\mathrm{arctanh}\left(\sqrt{\frac{w^2-a_0^2}{\eta^2-a_0^2}}\right), \tag{13}$$

$$a_0 \to w\sqrt{1-(I_0/I_{c1})^2}, \tag{14}$$

$$\varphi(u) \to \sqrt{\frac{w^2-a_0^2}{|u^2-a_0^2|}}. \tag{15}$$

Equations (13)–(15) correspond to the expressions for a flat superconducting tape.[1,3,4]

Figure 6 shows plots of the sheet current $K_z(u)$ from Eq. (11) and the perpendicular field $H_v(u,0)$ from Eq. (10). The sheet current K_z becomes more uniform as θ_1 approaches $\pi/2$, and the perpendicular field H_v for a curved tape is smaller than that for a flat tape.

C. ac loss in a single curved tape

Here we consider the response of a curved superconducting tape to an ac transport current $I_z=I_{p1}\cos\omega t$. Integrating Faraday's law, the electric field $E_z(u)$ at $\zeta=iR(1-e^{iu/R})$ in a curved tape is obtained from the perpendicular field $H_v(u,0)$ as

$$E_z(u) = -\frac{d}{dt}\int_0^u du'\,\mu_0 H_v(u',0). \tag{16}$$

The ac loss Q_1 in a curved superconducting tape per unit length is, thus, given by[13]

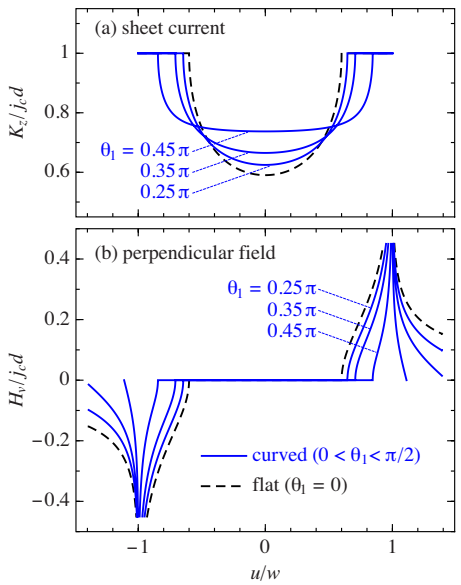

FIG. 6. (Color online) Distributions of (a) the sheet current $K_z(u)$ and (b) the perpendicular field $H_v(u,0)$ for $I_0/I_{c1}=0.8$ in a flat superconducting tape with $\theta_1=0$ (dashed line) and those in a curved superconducting tape with $\theta_1=0.25\pi$, 0.35π, and 0.45π (solid lines).

$$Q_1 = 8\mu_0 j_c d \int_{a_0}^{w} du(w-u)H_v(u,0), \tag{17}$$

where $H_v(u,0)$ is the perpendicular field when the transport current is at the maximum (i.e., $I_z=+I_{p1}$) in the ac cycle. Substituting Eqs. (7), (10), and (12) into Eq. (17), with I_0 replaced by I_{p1}, we have

$$Q_1 = \frac{\mu_0 I_{c1}^2}{\pi} F^2 \int_0^1 ds(1-2s)\ln\left[1-\frac{\tan^2(sF\theta_1)}{\tan^2\theta_1}\right], \tag{18}$$

where $F=I_{p1}/I_{c1}$ and $\theta_1=w/2R$. This expression for the ac loss in a single curved superconducting tape is equivalent to that for an infinite array of coplanar tapes.[11,14]

When the logarithmic function in Eq. (18) is expanded as $\ln(1-\tau_1)\simeq-\tau_1$, where $\tau_1=\cot^2\theta_1\tan^2(sF\theta_1)\ll 1$, we obtain

$$Q_1 \simeq \frac{\mu_0 I_{c1}^2}{\pi}\frac{\cot^2\theta_1}{\theta_1^2}\{2\ln[\cos(F\theta_1)]+F\theta_1\tan(F\theta_1)\}, \tag{19}$$

which is accurate for small F and large θ_1. When $0<F<0.8$ and $0.4\pi<\theta_1<0.5\pi$, the relative error in Eq. (19) compared to Eq. (18) is less than 10%.

For $\theta_1\to 0$, Eq. (18) reduces to the ac loss in a flat superconducting tape as given by Norris.[1] For small currents, $F=I_{p1}/I_{c1}\ll 1$, Eqs. (18) and (19) reduce to[11,14]

$$Q_1 \simeq \frac{\mu_0 I_{c1}^2}{6\pi} F^4 \theta_1^2 \cot^2\theta_1. \tag{20}$$

The distance between the edges of a curved tape, $2g=2R\sin(w/R)\simeq 2\pi R-2w$, becomes small when $\theta_1\to\pi/2$. For a small gap, $g/w\ll 1-F$, Eqs. (18) and (19) reduce to

$$Q_1 \simeq \frac{\mu_0 I_{c1}^2}{\pi}\left(\frac{g}{w}\right)^2\left\{2\ln\left[\cos\left(\frac{\pi F}{2}\right)\right]+\frac{\pi F}{2}\tan\left(\frac{\pi F}{2}\right)\right\}, \tag{21}$$

which is equivalent to the ac loss in two semi-infinite superconducting films with a gap.[15]

Note that Eqs. (16)–(21) are valid when $2g$ is much larger than d because the contribution of the penetration of the parallel field H_u is neglected in those expressions. On the other hand, when $2g\sim d$, the contribution of the parallel field H_u cannot be neglected when evaluating the ac losses. In this case the contributions of both the perpendicular field H_v and the parallel field H_u (i.e., "edge losses" and "top and bottom losses"[16]) should be included.

For zero gap $2g=0$ (i.e., $\theta_1=\pi/2$), a curved tape becomes a hollow cylinder, in which the perpendicular field is zero (i.e., $H_v=0$) and the ac loss is determined by the penetration of the parallel field H_u. The corresponding ac loss, based on the monoblock model,[17] is given by

$$Q_m = \frac{\mu_0 I_{c1}^2}{\pi h^2}\left[\left(1-\frac{hF}{2}\right)hF+(1-hF)\ln(1-hF)\right], \tag{22}$$

where $h=1-(1-d/R)^2$. When the tape thickness d is much smaller than the radius R, we have $h\simeq 2d/R\ll 1$ and Eq. (22) reduces to[18]

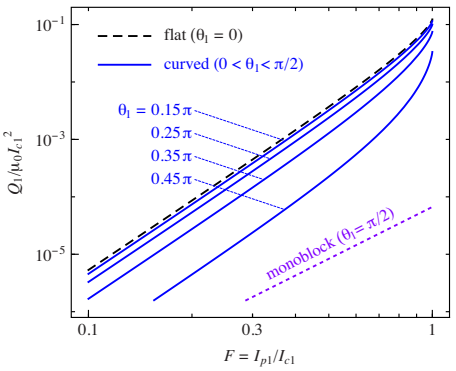

FIG. 7. (Color online) The ac loss Q_1 in a curved superconducting tape per unit length as a function of the normalized current amplitude $F=I_{p1}/I_{c1}$. Q_1 is shown for a flat tape with $\theta_1=0$ (dashed line), curved tapes with $\theta_1=0.15\pi$, 0.25π, 0.35π, and 0.45π (solid lines), and a monoblock model with $\theta_1=\pi/2$ (dotted line).

$$Q_m \simeq \frac{\mu_0 I_{c1}^2}{3\pi}\frac{d}{R}F^3. \tag{23}$$

Figure 7 shows the ac loss Q_1 in a curved superconducting tape carrying an ac transport current of amplitude I_{p1}. The dashed line shows Q_1 for a flat tape ($\theta_1=0$) and the solid lines show Q_1 for curved tapes with $\theta_1=0.15\pi$, 0.25π, 0.35π, and 0.45π obtained from Eq. (18). The dotted line shows $Q_1=Q_m$ of the monoblock model for $\theta_1=\pi/2$ and is obtained from Eq. (22) with $d/2w=10^{-4}$ (e.g., $d=1$ μm and $2w=10$ mm).

III. NUMBER OF CURVED TAPES AROUND A CYLINDER

A. Geometry of curved tapes around a cylinder

In this section we consider n curved superconducting tapes of width $2w$ arranged on a cylinder of radius R, where $R>nw/\pi$, as shown in Fig. 8. As suggested by Amemiya *et al.*,[6] the ac loss in such a round cable is expected to be smaller than that of an angular cable with flat tapes as shown in Fig. 1 in Ref. 14.

B. Field distributions for multiple tapes arranged around a cylinder

By using the conformal mapping in Eq. (1), the tapes which are curved in the ζ plane as shown in Fig. 8 are mapped onto an infinite array of coplanar tapes in the η plane (as shown in Fig. 3), where the periodicity of the coplanar array is $2\pi R/n$ rather than $2\pi R$.

The Biot-Savart law for the sheet current $K_z(u)$ and the complex field $\mathcal{H}(\zeta)$ is given by

$$\mathcal{H}(\zeta) = \frac{1}{2\pi}\int_{-w}^{+w} du' \sum_{k=1}^{n} \frac{K_z(u')}{\zeta - iR[1-e^{i(u'/R+2\pi k/n)}]} = \frac{1}{2\pi}\int_{-w}^{+w} du' \frac{n(\zeta-iR)^{n-1}K_z(u')}{(\zeta-iR)^n-(-iRe^{iu'/R})^n}. \tag{24}$$

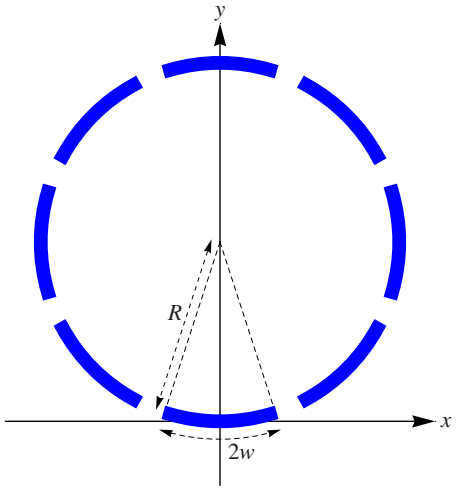

FIG. 8. (Color online) Superconducting tapes of width $2w$ are periodically arranged around a cylinder of radius R (where $R > nw/\pi$). The important parameter characterizing the n tapes is $\theta_n = nw/2R$, where $0 < \theta_n < \pi/2$. This figure shows the cross section for $n=8$ tapes.

Substitution of Eqs. (1) and (24) into Eq. (2) yields

$$\tilde{\mathcal{H}}(\eta) = \frac{n}{2\pi R}\int_{-w}^{+w} du' \frac{iK_z(u')}{1 - e^{in(u'-\eta)/R}}, \tag{25}$$

which is obtained from Eq. (4) by making the replacement $R \to R/n$ (i.e., $\theta_1 \to \theta_n = nw/2R$). The resulting complex field $\tilde{\mathcal{H}}(\eta)$, the flux front parameter a_0, and the function for field distributions $\varphi(u)$ are, therefore, simply obtained by replacing R with R/n in Eqs. (6), (7), and (12), respectively.

C. ac loss in multiple tapes arranged around a cylinder

Here we consider the case where the superconducting tapes carry a total ac transport current $I_z = I_p \cos \omega t$. The ac loss in each tape, Q_n/n, is also simply obtained from Q_1 in Eq. (18) by making the replacement $R \to R/n$, and the total ac loss in curved tapes Q_n is given by

$$Q_n = \frac{\mu_0 I_c^2}{\pi n} F^2 \int_0^1 ds(1-2s)\ln\left[1 - \frac{\tan^2(sF\theta_n)}{\tan^2 \theta_n}\right], \tag{26}$$

where $\theta_n = nw/2R$, $F = I_p/I_c = I_{p1}/I_{c1}$, $I_p = nI_{p1}$ is the amplitude of total current, and $I_c = nI_{c1} = 2nj_c wd$ is the total critical current.

When the logarithmic function in Eq. (26) is expanded as $\ln(1-\tau_n) \simeq -\tau_n$, where $\tau_n = \cot^2 \theta_n \tan^2(sF\theta_n) \ll 1$, we obtain

$$Q_n \simeq \frac{\mu_0 I_c^2}{\pi n}\frac{\cot^2 \theta_n}{\theta_n^2}\{2 \ln[\cos(F\theta_n)] + F\theta_n \tan(F\theta_n)\}, \tag{27}$$

which is accurate for small F and large θ_n.

For $\theta_n \ll 1$, both the bending effect and the interaction among superconducting tapes can be neglected, and Eq. (26) reduces to the expression given by Norris,[1]

$$Q_n \simeq \frac{\mu_0 I_c^2}{\pi n}[(1+F)\ln(1+F) + (1-F)\ln(1+F) - F^2]. \tag{28}$$

For small currents, $F = I_p/I_c \ll 1$, Eqs. (26) and (27) reduce to[11,14]

$$Q_n \simeq \frac{\mu_0 I_c^2}{6\pi n} F^4 \theta_n^2 \cot^2 \theta_n. \tag{29}$$

The gap between the edges of the tapes is given by $2g = 2R \sin(\pi/n - w/R)$ and can be approximated as $2g \simeq 2\pi R/n - 2w$ for $1 - nw/\pi R \ll 1$. For small gaps, $g/w \ll 1 - F$, Eqs. (26) and (27) reduce to

$$Q_n \simeq \frac{\mu_0 I_c^2}{\pi n}\left(\frac{g}{w}\right)^2 \left\{2 \ln\left[\cos\left(\frac{\pi F}{2}\right)\right] + \frac{\pi F}{2}\tan\left(\frac{\pi F}{2}\right)\right\}, \tag{30}$$

which is proportional to $(I_c^2/n)(g/w)^2 = n(2g)^2 j_c^2 d^2$ when $F = I_p/I_c$ is fixed. Furthermore, when $F = I_p/I_c$, $j_c d$, $2g$, and $I_c \propto 2nw$ are all fixed, Eq. (30) shows that $Q_n \propto n \propto 1/2w$, which suggests that *the small number of wide tapes* is an advantageous design for reducing total ac loss in curved superconducting tapes arranged around a cylinder. For zero gap $2g = 0$ (i.e., $\theta_n = \pi/2$), Eqs. (26)–(30) are not valid, and the ac loss corresponds to the monoblock model result given by Eq. (22).

IV. SUMMARY

We investigated theoretically the field distributions and ac losses in curved superconducting tapes with the shape of a section of a cylindrical shell. The current and magnetic field distributions in curved superconducting tapes (as shown in Figs. 2 and 8) carrying transport currents are equivalent to those of an infinite array of coplanar superconducting tapes (as shown in Fig. 3).

The current and field distributions for a single curved superconducting tape (as shown in Fig. 2) carrying a transport current are given by Eqs. (6)–(12). The ac loss Q_1 in a single curved superconducting tape carrying an ac transport current is given by Eq. (18) with an approximate expression given by Eq. (19). Bending superconducting tapes reduces both the perpendicular magnetic field and the ac loss.

The expressions for the current and field distributions due to a number of curved superconducting tapes arranged regularly around a cylinder (as shown in Fig. 8) are obtained simply by making the replacement $R \to R/n$ in the corresponding expressions for a single curved tape. The total ac loss Q_n in a number of curved superconducting tapes conforming to a cylinder and carrying ac transport currents is given by Eq. (26) with an approximate expression given by Eq. (27). Equation (30) for the small gap limit suggests that a small number of wide tapes is an advantageous design for reducing ac losses in a round cable surrounded by curved superconducting tapes.

ACKNOWLEDGMENTS

I thank A. P. Malozemoff for stimulating and fruitful discussions. I also thank Y. Shiohara, T. Izumi, K. Tanabe, N. Fujiwara, and H. Yamasaki for their encouraging comments and support. This work was supported by the New Energy and Industrial Technology Development Organization (NEDO) as part of the M-PACC Project (Materials and Power Application of Coated Conductor Project).

[1] W. T. Norris, J. Phys. D **3**, 489 (1970).
[2] M. R. Halse, J. Phys. D **3**, 717 (1970).
[3] E. H. Brandt, M. V. Indenbom, and A. Forkl, Europhys. Lett. **22**, 735 (1993); E. H. Brandt and M. Indenbom, Phys. Rev. B **48**, 12893 (1993).
[4] E. Zeldov, J. R. Clem, M. McElfresh, and M. Darwin, Phys. Rev. B **49**, 9802 (1994).
[5] M. Yagi, S. Mukoyama, N. Amemiya, N. Kashima, S. Nagaya, and Y. Shiohara, Supercond. Sci. Technol. **22**, 085003 (2009).
[6] N. Amemiya *et al.*, in Extended Abstracts of the Ninth International Workshop on Coated Conductors for Applications (CCA-08) (unpublished) (http://ewh.ieee.org/tc/csc/europe/newsforum/abstract-CCA08-3F.03.html).
[7] C. P. Bean, Phys. Rev. Lett. **8**, 250 (1962); Rev. Mod. Phys. **36**, 31 (1964).
[8] L. D. Landau and E. M. Lifschitz, *Electrodynamics of Continuous Media, Theoretical Physics* (Pergamon, Oxford, 1963), Vol. 8.
[9] R. A. Beth, J. Appl. Phys. **37**, 2568 (1966).
[10] Y. Mawatari, Phys. Rev. B **54**, 13215 (1996).
[11] Y. Mawatari, in *Advances in Superconductivity IX*, edited by S. Nakajima and M. Murakami (Springer, Tokyo, 1997), p. 575.
[12] K.-H. Müller, Physica C **289**, 123 (1997).
[13] J. R. Clem, J. H. Claassen, and Y. Mawatari, Supercond. Sci. Technol. **20**, 1130 (2007).
[14] Y. Mawatari and K. Kajikawa, Appl. Phys. Lett. **92**, 012504 (2008).
[15] M. Majoroš, Physica C **272**, 62 (1996).
[16] J. R. Clem, Phys. Rev. B **77**, 134506 (2008).
[17] G. Vellego and P. Metra, Supercond. Sci. Technol. **8**, 476 (1995).
[18] A. P. Malozemoff, G. Snitchler, and Y. Mawatari, IEEE Trans. Appl. Supercond. **19**, 3115 (2009).